Modeling of radiation spur processes in water at temperatures up to 300 ∘ C. J Phys Chem

ARTICLE *in* THE JOURNAL OF PHYSICAL CHEMISTRY · JULY 1995

Impact Factor: 2.78 · DOI: 10.1021/j100029a026

2 AUTHORS, INCLUDING:

Dorota Swiatla-Wojcik
Lodz University of Technology
40 PUBLICATIONS **407** CITATIONS

SEE PROFILE

Modeling of Radiation Spur Processes in Water at Temperatures up to 300 °C

Dorota Swiatla-Wojcik

Technical University of Lodz, Institute of Applied Radiation Chemistry, 90-924 Lodz, Zwirki, Poland

George V. Buxton*

Cookridge Radiation Research Centre, University of Leeds, Cookridge Hospital, Leeds LS16 6QB, U.K.

Received: May 17, 1995[⊗]

Deterministic diffusion-kinetic modeling has been performed to calculate the temperature dependence of the radiation chemical yields (G-values) of the radiolysis products of water. The FACSIMILE numerical method has been used to solve a set of coupled differential equations describing the diffusion and reactions of the species for the temperature range 20−300 °C. The low LET spherically symmetrical case of an "average" spur with 62.5 eV deposited in it has been considered. Modeling calculations have been compared for Gaussian, an exponential distribution, and a distribution with a central minimum assumed as the initial spatial distribution of the hydrated electron (e_{aq}^-). In all cases spatial distributions of the other radiolytic products started as Gaussian. To fit the experimental data it has been necessary to assume that the reaction $e_{aq}^- + e_{aq}^- \rightarrow H_2 + 2OH^-$ becomes diffusion controlled at elevated temperatures and to include a contribution of 13% to the initial yields of water decomposition through the dissociation of electronically and vibrationally excited molecules: $H_2O^* \rightarrow H + OH$ (I) and $H_2O^* \rightarrow H_2 + O(^1D) \rightarrow H_2 + 2OH$ (or H_2O_2) (II). The products of these processes are considered to be correlated in space. Good accord with experiment is achieved with the total contributions of I and II being independent of temperature but with their ratio decreasing from ca. 21:1 to ca. 4:1 with increasing temperature above 220 °C. For process I calculations predict a temperature dependent probability of cage recombination of H + OH. For process II slightly better agreement is obtained with the solvolysis of $O(^1D)$ producing H_2O_2 instead of a caged pair of OH's.

Introduction

Corrosion processes in water-cooled nuclear power reactors (PWRs) are associated with the radiolysis of the coolant at ca. 300 °C. To predict the effects of radiation, it is necessary to know chemical yields of oxidizing and reducing radiolytic products. Radiation chemical yields of the species can be estimated by addition of solutes which react selectively with the desired radical to form a measurable product. There are two main limitations in the choice of a suitable experimental system. The solute and the product should be stable at ambient and elevated temperatures if steady state radiolysis is employed. It is not the case in the pulse radiolysis method which allows a measurable product to be a transient one. In that case, however, knowledge of the extinction coefficient at temperatures up to 300 °C is required to obtain reliable information about the *G*-values. As a result of the above limitations, the chemical yields for some of the radiolytic products at reactor temperatures (ca. 300 °C) are unknown. Attempts have been made to estimate high-temperature *G*-values on the basis of those measured at lower temperatures.[1] Such extrapolation, however, may produce rather crude or even wrong values. In that situation the numerical modeling of spur processes presents a complementary method for estimation of the *G*-values in the experimentally inaccessible region.

Many of the theories for low-LET (linear energy transfer) radiolysis assume the energy deposition occurs in localized well-separated regions of spherical symmetry, called spurs.[2,3] In pure water each spur contains a number of reactive species: e_{aq}^-, H, OH, H_2, H_2O_2, and H^+. The radiolytic products can either react within the spur or escape reaction and diffuse out into the bulk. The radiation chemical yields which are of interest here result from the latter.

Rates of diffusion and reaction are known to be temperature dependent. The temperature dependences of the diffusion coefficients and reaction rate constants have been studied recently for the majority of the radiolytic products.[4−11] However, the effect of temperature on the structure of spurs is unknown. Diminution of hydrogen bonding at elevated temperatures may affect primary processes such as the decomposition of excited water molecules, thermalization of the fragments, cage recombination, etc., leading to changes in the number of radicals and their distribution within the spurs. These effects can be examined by applying various assumptions in modeling calculations and comparing the calculated yields of products with data from experiments.

Recently, LaVerne and Pimblott[12] have employed the deterministic diffusion-kinetic approach[13,14] to show how scaling of the initial spur radii with temperature affects the calculated *G*-values. Their best fit obtained for an activation-controlled increase of the initial spur radius of e_{aq}^- from 2.3 nm at room temperature to 5.8 nm at 300 °C and a temperature independent spur radius of 0.85 nm for the other species reasonably matches the experimental data up to 150 °C. Above 150 °C the calculations underestimate the *G*-values of the hydroxyl radical and molecular hydrogen and predict a decrease in $G(H_2)$ instead of the observed increase.[1] LaVerne and Pimblott[12] did not regard the major disagreement which they noted between the calculated and measured values of $G(H_2)$ at high temperatures as significant "considering the large discrepancy between the different sets of experimental data". However, they included a data set which is judged by Elliot *et al.*[1] to be invalid. LaVerne and Pimblott[12] further noted that at 300 °C their diffusion-kinetic model predicts a value of $G(H_2)$ which is three-fold lower than

* To whom correspondence should be addressed.

[⊗] Abstract published in *Advance ACS Abstracts,* July 1, 1995.

0022-3654/95/2099-11464$09.00/0

TABLE 1: Reaction Scheme of the Chemical Stage in Water Radiolysis

symbol	reaction
R1	$e_{aq}^- + H^+ \rightarrow H$
R2	$e_{aq}^- + OH \rightarrow OH^-$
R3	$H^+ + OH^- \rightarrow H_2O$
R4	$e_{aq}^- + e_{aq}^- \rightarrow H_2 + 2OH^-$
R5	$e_{aq}^- + H \rightarrow H_2 + OH^-$
R6	$H + H \rightarrow H_2$
R7	$H + OH \rightarrow H_2O$
R8	$OH + OH \rightarrow H_2O_2$
R9	$e_{aq}^- + H_2O_2 \rightarrow OH^- + OH$

the experimental value that Elliot *et al.*[1] consider to be a reliable one. It was suggested[12] that the use of a stochastic model would probably give better results for the molecular yields. In comparison with deterministic calculations, however, stochastic treatments were shown to predict lower *G*-values of molecular products[15] and it seems that other factors may be responsible for the major disagreement between calculated[12] and measured[1] values of $G(H_2)$ at elevated temperatures.

LaVerne and Pimblott[12] assumed that the reaction between e_{aq}^- and OH is diffusion controlled whereas it is now known to be activation controlled.[9] This reaction plays a crucial role in the spur decay of e_{aq}^- and OH so that use of the correct temperature dependence of the rate constant is expected to change the results. Also, the rate constants for the reaction of e_{aq}^- with H which have recently been reported[11] should be incorporated in the modeling calculations.

Although the work by LaVerne and Pimblott[12] leaves room for improvements in predicting radiation chemical yields at temperatures pertinent to PWRs, it showed that the deterministic model can be considered as an efficient tool in elucidating and examining spur processes in water at elevated temperatures.

The present paper aims to improve the physical and chemical picture of spur processes in water at elevated temperatures within the framework of the deterministic model. We have examined two decomposition mechanisms for excited water molecules with cage recombination of the decomposition fragments, as well as the temperature dependence of the rate constant for the reaction $e_{aq}^- + e_{aq}^- \rightarrow H_2 + 2OH^-$. In this work various schemes of radiolysis have been considered to account for the initial unscavengeable yield of molecular hydrogen and calculations have been performed with updated rate constants for the reactions $e_{aq}^- + OH \rightarrow OH^-$ (ref 9) and $e_{aq}^- + H \rightarrow H_2 + OH^-$.[11] Also, the initial spur size has been scaled according to the density changes of the system. In the following section the reaction scheme and the numerical procedure are presented. The assumptions on the temperature dependence of spur parameters, diffusion coefficients, and reaction rate constants are described in the third section. Later on the results of our modeling are discussed and compared with the available experimental data. We conclude with a short summary and final remarks.

Numerical Method and Reaction Scheme

To model the radiation chemistry in a low-LET electron track, we followed the deterministic approach and adopted the concept of an average isolated spherical spur with 62.5 eV deposited in it.[12-14] The application of this average spur model has been discussed in detail by LaVerne and Pimblott,[14] who have shown that it represents quite well experimental yields measured at room temperature using scavengers. Our modeling concerns the radiation chemical stage, i.e. the time period from 10^{-12} s, when the ionization, dissociation, and thermalization events are complete, to 10^{-6} s, when molecular or secondary radical products have been formed and diffused out of the spur. The

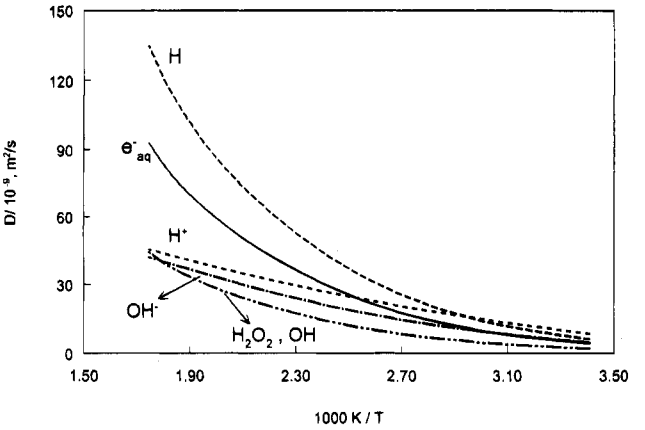

Figure 1. Diffusion coefficients for the reactive species as a function of reciprocal absolute temperature.

TABLE 2: Diffusion Coefficients at Room Temperature

i	species	D_i (25 °C) [10^9 m²/s]	ref
1	H_2O	2.31	21, 22
2	e_{aq}^-	4.82	22, 23
3	H	7.0	23
4	OH	2.31	*a*, 23
5	H_2O_2	2.31	*a*

[a] Assumed to be the same as that for water.[21]

reaction scheme of the chemical stage in water includes the 9 reactions listed in Table 1. It was found that other reactions involved in the radiolysis of water do not affect the yields of products at 10^{-6} s over the whole temperature range.

The spur diffusion model has been assumed for the whole range of temperature. According to the model, at the beginning of the chemical stage the primary species begin to diffuse and encounter one another. Some of them react together to form the radiolytic products which in turn diffuse out of the spur. The others escape into the bulk and become homogeneously distributed throughout the medium. A numerical formulation of the spur diffusion concept was initially proposed by Schwarz[16] and extended by Burns *et al.*[17] In order to model the time evolution of an "average" spur, the set of coupled differential equations describing diffusion and reactions of the species has been solved by means of the FACSIMILE program.[18] We followed the numerical procedure,[13] which divides reaction space into a number of concentric zones into each of which the reactants are placed according to the required spatial distribution. Most of the results presented in this paper were obtained for the Gaussian distribution. To maintain the mass flowing into the outermost zone negligible at high temperatures, the number of $n = 54$ zones was assumed.

To analyze the FACSIMILE output in the whole temperature range and include our assumptions on spur parameters (cf. next section), the original algorithm has been modified and the subsidiary programs have been worked out in FORTRAN.

The radiation chemical yields of the oxidizing (OH, H_2O_2) and reducing (e_{aq}^-, H, H_2) species have been calculated for temperatures $t = i \times 20$ °C, where $i = 1, 2, ..., 15$. The *G*-values are expressed in molecule/100 eV.

Data Set. To calculate the *G*-values of the oxidizing and reducing species, the following data set is required for each temperature.

Diffusion Coefficients. In Figure 1 the diffusion coefficients are shown as functions of temperature. The temperature dependences for H^+ and OH^- represent the polynomial fit to the experimental data.[19,20] For the other species the scaling

TABLE 3: Parameters for Reactions Whose Rates Were Calculated on the Basis of Eq 2

reaction A + B as in Table 1	r_A [nm]	r_B [nm]	E_{act} [kJ/mol]	k_{act} (25 °C) [10^{10} M^{-1} s^{-1}]	β	temperature range of reported rates [°C]	comments
R1	0.8[a]	0.25[5]	10.0[a]	2.37[a,b]	1[5]	20−200[5]	assumed partially diffusion controlled (PDF)[i]
R2	0.8[a]	0.22[23]	0.0[a]	6.4[a,c]	1[a]	18−150[9]	PDF[a]
						20−225[11]	
R3	0.25[5]	0.33[d]	0.0[a]	10^3 [a]	1[a]	0−48[7]	assumed diffusion controlled (DF)[7 a]
R4	0.8[a]	0.8[a]	30.0[a]	1.3[a,b]	0.25[a]	5−300[10]	PDF[a,g]
						20−150[e]	
R5	0.8[a]	0.19[6]	0.0[a]	110[a]	0.25[a]	25[26,27]	DF[g]
						20−250[11]	
						20−250[f]	
R6	0.19[6]	0.19[6]	0.0[6]	10^3 [6]	0.25[6]	18−250[8]	DF[6]
R7	0.19[6]	0.22[6,23]	0.0[6]	3.58[6 c]	1[6]	20−200[6]	PDF[6]
R8	0.22[6,23]	0.22[6,23]	0.0[6]	1.0[6 c]	1[5,6]	20−200[5]	PDF[5,6]
R9	0.8[a]	0.21[5]	15.5[a]	1.8[a]	1[5]	20−200[5]	PDF[a,h]
						0−150[11]	

[a] This work. [b] Pre-exponential factor A does not depend on temperature. [c] $A = A'T$. [d] Estimated from the reaction distance $r = 0.58$ nm.[7] [e] Data from ref 10 recalculated using extinction coefficient data for e_{aq}^- from ref 9. [f] Data from ref 11 recalculated using extinction coefficient data for e_{aq}^- from ref 9. [g] Fitted to the experimental data corrected for changes in extinction coefficient. [h] Fitted to the experimental data.[11] [i] These parameters have been derived from data communicated by Dr. A. J. Elliot.

procedure[5,12] has been adopted:

$$D_i(t) = [D_i(25\ °C)/D_{H_2O}(25\ °C)]D_{H_2O}(t) \quad (1)$$

where t denotes the temperature in Celsius. The diffusion coefficients D_i (25 °C) at room temperature are given in Table 2.

The temperature dependence for D_{H_2O} up to 225 °C was taken from ref 21 and extrapolated to 300 °C by the Stokes−Einstein relationship using the viscosity of water.

Reaction Rate Constants. As shown elsewhere[5,6] a valuable method for a mathematical presentation of the measured rate constants is based on the Noyes relation[24]

$$1/k = 1/k_{diff} + 1/k_{act} \quad (2)$$

Here the reciprocal measured value is represented by the sum of the diffusion and the activation part. The temperature dependence of k_{diff} is given by the Smoluchowski equation

$$k_{diff}(t) = 4\pi N D(t) r \beta f_D(t) \quad (3)$$

where N is Avogadro's number, D is the sum of diffusion coefficients, r is the reaction distance, i.e. the sum of the reaction radii, β is the statistical spin factor as discussed in refs 5 and 6, and f_D denotes the Debye factor. When the reactants A and B are both ions, $f_D = \delta/(e^\delta - 1)$ is not equal to unity and depends on temperature via the relation

$$\delta = Z_A Z_B e^2/(4\pi\epsilon_0\epsilon(t) r k_B T) \quad (4)$$

where Z_A and Z_B are the charges on the ions, ϵ_0 is the permittivity of free space, $T = 273 + t$, and ϵ is the dielectric constant of the medium. The values of $\epsilon(t)$ for pure water were taken from ref 25.

The Arrhenius equation was used[5,6] to evaluate k_{act} empirically

$$k_{act} = A \exp(-E_{act}/RT) \quad (5)$$

Either the temperature independent form[5] or $A = A'T$ (ref 6) has been taken for the pre-exponential factor A. All parameters used to fit the measured rate constants are listed in Table 3. In Figure 2 the calculated rate constants are shown for the temperature range 20−300 °C.

The temperature dependences of the rate constants have been reported for the reactions: R1,[5] R2,[9,11] R3,[7] R4,[10] R5,[11] R6,[8]

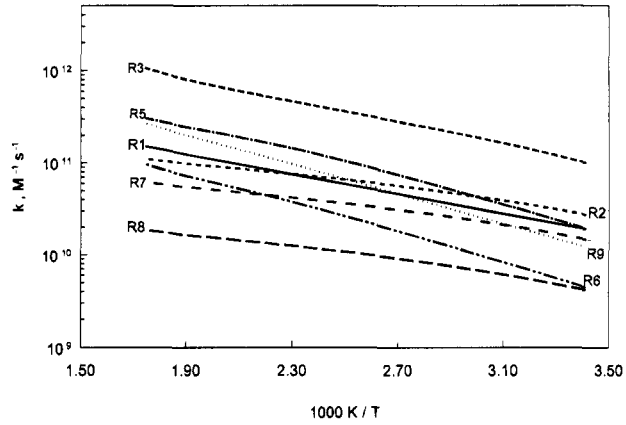

Figure 2. Rate constants for the spur reactions shown in Table 1 as a function of reciprocal absolute temperature.

R7,[6] R8,[5] and R9.[5,11] Except for R4 they show an increase in the rate constants with increasing temperature. As reported by Christensen and Sehested[10] the rate constant of the self reaction of e_{aq}^- exhibits a maximum at about 150 °C. The authors explain this result in terms of the dielectron $(e_2^{2-})_{aq}$ as an intermediate which either decays to form molecular hydrogen or undergoes a reverse reaction as below:

$$e_{aq}^- + e_{aq}^- \leftrightarrow (e_2^{2-})_{aq} \rightarrow H_2 + 2OH^- \quad (6)$$

Christensen and Sehested[10] obtained their data under alkaline conditions, so there may have been a competition between protonation and dissociation of the dielectron. Under our conditions the spur is acidic and it seems possible that the dielectron may protonate to give the same intermediate as for reaction R5. When the data of Christensen and Sehested[10] for reaction R4 are used, the temperature dependent G-values $G_H(t)$, $G_{H_2}(t)$, and $G_{e_{aq}^-}(t)$, calculated previously for Gaussian distributions of different width,[12] and those calculated in this work for Gaussian, exponential, and central minimum[28] spatial distributions of e_{aq}^- show a characteristic inflection at 150 °C which is not observed experimentally. Christensen and Sehested assumed that the extinction coefficient of e_{aq}^- at its absorption maximum is independent of temperature whereas Elliot[9] finds that it decreases with increasing temperature and so modifies the rate constants reported[10] for reaction R4. These modified values up to 150 °C are shown in Figure 3; in our modeling we have used values given by the solid line which is obtained from

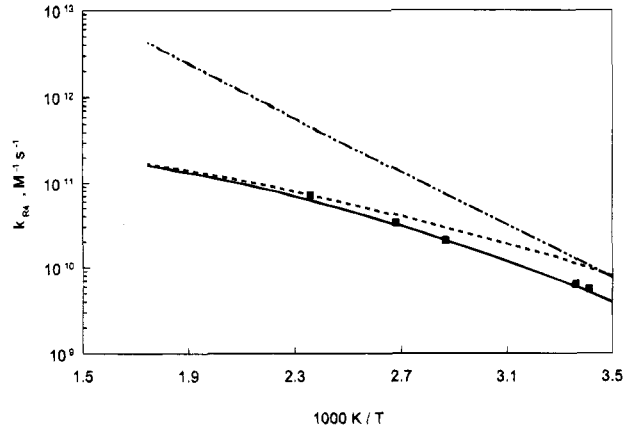

Figure 3. Rate constant of reaction R4 calculated from eq 2 versus reciprocal absolute temperature (—). Also shown are k_{diff} from eq 3 (- - -), k_{act} from eq 5 (— - - —), and experimental data from ref 24 recalculated using extinction coefficient data for e_{aq}^- from ref 23 (■).

applying eq 2 to the modified data. We believe that this is a reasonable approach, and it seems to be justified by the agreement we have obtained between model and experiment. Our values of the rate constants for reactions R2 and R4 are significantly different from those used by LaVerne and Pimblott.[12]

The reaction radius of 0.8 nm for e_{aq}^- has been derived from applying the values of reported rate constants to eq 2 and assuming a statistical spin factor equal to 1 for reactions R1, R2, and R9 and 0.25 for R4 and R5.

Spur Parameters. At the end of the physical stage ($\sim 10^{-15}$ s) the low-LET track in liquid water contains H_2O^+, subexcitation electrons, e_{se}^-, and electronically excited water molecules, H_2O^*.[2,3,29,30] The primary species which take part in the chemical stage of the radiolysis are formed during the physicochemical stage from about 10^{-15} to 10^{-12} s. To include all the processes considered in various models of the radiolysis of liquid water, the physicochemical stage can be described by the following scheme:

$$e_{se}^- + H_2O^+ \longrightarrow$$

$$H_2O^*_{vib} \longrightarrow \begin{cases} OH + H & \text{(Ia)} \\ H_2 + O(^1D) \xrightarrow{H_2O} H_2 + 2OH \text{ (or } H_2O_2) & \text{(Ib)} \\ 2H + O(^3P) & \text{(Ic)} \end{cases}$$

$$H_2O^+ \xrightarrow{H_2O} H^+_{aq} + OH \quad \text{(II)}$$

$$e_{se}^- + H_2O \rightarrow OH + H^- \xrightarrow{H_2O} OH + H_2 + OH^- \quad \text{(III)}$$

$$e_{se}^- + H_2O \rightarrow e_{aq}^- \quad \text{(IV)}$$

$$H_2O^* \longrightarrow \begin{cases} OH + H & \text{(Va)} \\ H_2 + O(^1D) \xrightarrow{H_2O} H_2 + 2OH \text{ (or } H_2O_2) & \text{(Vb)} \\ 2H + O(^3P) & \text{(Vc)} \end{cases}$$

In most cases in the previous models[12,14-16] recombination of dry electrons with their parent cations (process I) was neglected, but it has been pointed out that this process is not negligible.[31,32] According to Kaplan *et al.*[32] process I produces water molecules in high vibrational levels of their electronic ground state. The remaining H_2O^+ reacts with water to form H_{aq}^+ and OH (process II) whilst the subexcitation electrons which escape process I either undergo a dissociative attachment to H_2O (process III) or thermalize and become solvated (process IV). Process III, which is important in the gas phase, was suggested by Platzman[33] and by Faraggi and Desalos[34] to be responsible for the unscavengeable yield of molecular hydrogen in the radiolysis of liquid water.

Since very little is known about the decay channels for excited water molecules in the liquid phase, we have based our interpretation on the data reported for the gas phase. Theoretical calculations for an isolated water molecule,[35] as well as experimental studies of water vapor,[36-38] indicate that there are three decay channels for electronically excited water molecules represented by processes Va, Vb, and Vc. The same processes have been reported to occur with the vibrationally excited molecules formed by recombination of e^- and H_2O^+ in the gas phase.[39]

Decomposition of electronically excited states into H and OH (process Va) has been included in previous models of the radiolysis of liquid water as the main source of the initial yield of the hydrogen atom.[12,14-16,32] Process Vb was included in Schwarz's modeling[16] and in the subsequent works[12-15,30,32] to account for an unscavengeable yield of H_2. Singlet oxygen, $O(^1D)$, resulting from this decomposition mechanism rapidly reacts with water and may increase the yield of OH or produce H_2O_2 (see below). The third decay channel (processes Ic and Vc) has not been considered in the modeling of the radiolysis of liquid water. A very small yield with $G(O(^3P)) \sim 0.0067$ has been reported by Brown and Hart[40] at long times in liquid water, which indicates that processes Ic and Vc are insignificant in this phase.

To calculate the content of an "average" spur, two yield parameters are involved: the initial yield of ionizations and the initial yield of excitations denoted here by $G°$(ion) and $G°$(ex), respectively. As discussed by LaVerne and Pimblott,[12] there is no reason to expect a change in the energy deposition with increasing temperature. The parameters $G°$(ion) and $G°$(ex) as well as the contributions of processes I–IV have been assumed to be temperature independent up to 300 °C.

In the calculation of $G°$(ion) in liquid water we have adopted the probabilities for the thermalization, recombination, and dissociative attachment of subexcitation electrons in amorphous solid water predicted by Monte Carlo simulation as 0.92, 0.047, and 0.033, respectively.[41] With the parameter $G°(e_{aq}^-) = 4.78$, which was reported in the earlier deterministic studies,[14,16] our calculation results in $G°$(ion) = 5.20 and, in consequence, $G°(H^+_{aq}) = 4.95$ and $G°(OH^-) = 0.17$.

The primary species which diffuse faster at elevated temperatures can be expected to escape spur reactions and result in higher radical yields and lower yields of the molecular products. This premiss has been confirmed by the previous[12] as well as by our modeling calculations. To explain an observed increase in $G(H_2)$, Burns and Marsh[42] and Elliot *et al.*[1] suggested thermally dependent decomposition of the electronically excited water molecules but, on the basis of their calculations, LaVerne and Pimblott[12] concluded that such a process is not required for their model predictions to match the experimental data.

In the present study the initial yield of molecular hydrogen $G°(H_2)$ has been divided into the temperature independent part $G°_1(H_2)$ (=0.17) resulting from process III and $G°_2(H_2)$, which originates from the decay of vibrationally and electronically excited molecules (processes Ib and Vb). In terms of the diminution of hydrogen bonding in liquid water at high temperatures, the efficiency of dissociation into $H_2 + O$ can be expected to approach that observed in water vapor. To account for a possible change in the relative contributions of the dissociation channels, we suggest a procedure called the

molecular hydrogen correction (MHC), which leads to the following temperature dependence of $G^\circ_2(H_2)$:

$$G^\circ_2(H_2)(t) = G^\circ_2(H_2)(25\ ^\circ C) + MHC(t) \quad (7)$$

$$MHC(t) = G_e(H_2)(t) - G^\circ_1(H_2) - G_s(H_2)(t) - G^\circ_2(H_2)(25\ ^\circ C) \quad (8)$$

where $G_e(H_2)(t)$ is the polynomial fitting to the experimental points,[1] $G_s(H_2)(t)$ represents the total yield of H_2 resulting from spur reactions R4, R5, and R6, and $G^\circ_2(H_2)(25\ ^\circ C)$ denotes the room temperature value of $G^\circ_2(H_2)$. This procedure increases the contribution of the H_2 + O channel in the total yield of dissociations but does not change the initial yield of excitations $G^\circ(ex)$.

The initial yields $G^\circ(ex)$ and $G^\circ_2(H_2)(25\ ^\circ C)$ of 0.73 and 0.03, respectively, have been obtained by adjustment of the G-values computed at 10^{-6} s to the observed yields of the radiolytic products. The MHC has been found to be significant in the temperature range 210−300 °C, where the total contribution of processes Ib and Vb increases from about 4.5% to 18%. In the gas phase, process Ib was reported to represent 21% of dissociative recombinations,[39] and process Vb to account for 10% of the photolysis yield at 121.6 nm.[38] The weighted average of the experimental data calculated with respect to the yield of processes I and V results in their contributions totalling 14%. The agreement with our value of 18% is quite satisfactory, taking into account that H atoms formed in the third decay channel (processes Ic and Vc), implicitly included in our approach, can partly recombine to result in H_2.

As pointed out in the previous works,[29,32] decomposition of excited molecules in the liquid phase can be associated with the so-called cage effect, i.e. the recombination of geminate pairs competing with escape of the radicals into the bulk liquid. The present study accounts for the cage recombination of OH and H resulting from the first decay channel and of two OH radicals resulting from the solvolysis reaction of $O(^1D)$ (processes Ib and Vb) rather than $O(^1D) + H_2$ recombination, which was assumed by Kaplan *et al.*[32] The reaction H_2 + O seems to be unlikely because O would have to insert in the H−H bond. On the other hand the solvolysis of singlet oxygen is very rapid. The rate constant in the gas phase for $O(^1D) + H_2O \rightarrow 2OH$ is 1.8×10^{10} dm^3 mol^{-1} s^{-1},[43] so in liquid water the half-life of $O(^1D)$ should be shorter than 1 ps. There are two pieces of experimental evidence supporting the formation of H_2O_2 in processes Ib and Vb. Firstly, in experiments performed with ^{18}O-labeled O_3 which was photolyzed to form $O(^1D)$, the product H_2O_2 was found to contain ca. 50% ^{18}O.[44] Taube[44] proposed that $O(^1D)$ inserts in H_2O to form H_2O_2, to account for the ^{18}O distribution, although the same distribution would result from recombination of a caged pair of OH's produced in processes Ib and Vb. Secondly, in the photodissociation process $H_2O_2 + h\nu(253.7\ nm) \rightarrow 2OH$ in liquid water, the quantum yield of OH was measured as 1.0.[45] In fact, whether we assume that $O(^1D)$ inserts in water to form H_2O_2 or produces a geminate pair of OH's makes very little difference to the calculated values of $G(OH)$ and $G(H_2O_2)$ (see Figure 6), although in the first case the probability of formation of H_2O_2 is 1.0 and in the second case it is 0.5. The "initial" G-value of H_2O_2 formed in processes Ib and Vb does not exceed 0.033 at 25 °C and would not be detectable experimentally.

In the dissociation of an excited water molecule into H + OH, any excess energy is mainly partitioned into translational energy of the fragments.[35,46] The maximum distance s_{max} which separates H and OH can be expressed as[32]

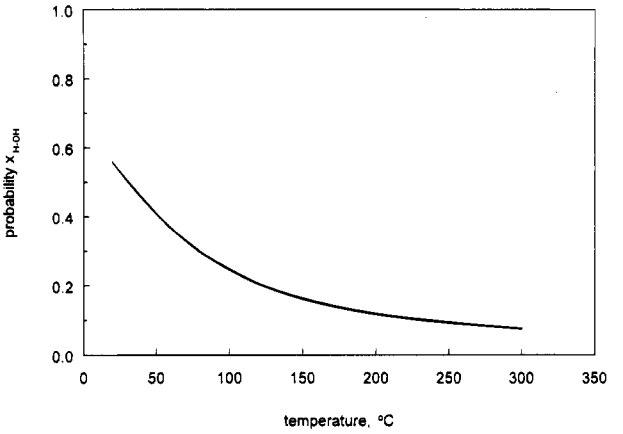

Figure 4. Probability x_{H-OH} of geminate recombination of H and OH (see text).

$$s_{max} = r_H + r_{OH} + \frac{1}{6\pi\eta}\left(\frac{(2m_H E_H)^{1/2}}{r_H} + \frac{(2m_{OH}E_{OH})^{1/2}}{r_{OH}}\right) \quad (9)$$

where η is the viscosity of the medium and r_H, r_{OH}, m_H, m_{OH}, E_H, and E_{OH} are the reaction radii, the masses, and the kinetic energies of the fragments, respectively. A decrease in viscosity from 1 cP at 25 °C to 0.09 cP at 300 °C[47] makes the separation distance longer, so a lowering of the probability of cage recombination can be expected with increasing temperature. In the calculation of the recombination probability of H + OH, we used eq 10:[48]

$$x_{H-OH} = \frac{(r_H + r_{OH})}{s_{max}} \frac{k_{act}}{k_{act} + k_{diff}} \quad (10)$$

The thermal dependence of the recombination probability x_{H-OH} is shown in Figure 4. Our value at room temperature is 0.53 compared with 0.51 obtained by Kaplan *et al.*[32]

The initial yields of the radiolytic products are connected by the following set of equations, with $x_{OH-OH} = 0.5$ or 1.0:

$$G^\circ(H^+_{aq}) = G^\circ(e^-_{aq}) + G^\circ_1(H_2) \quad (11)$$

$$G^\circ(H_2) = G^\circ_1(H_2) + G^\circ_2(H_2) \quad (12)$$

$$G^\circ(H) = [G^\circ(ex) - G^\circ_2(H_2)](1 - x_{H-OH}) \quad (13)$$

$$G^\circ(OH) = G^\circ(H^+_{aq}) + G^\circ(H) + G^\circ_1(H_2) + 2(1 - x_{OH-OH})G^\circ_2(H_2) \quad (14)$$

$$G^\circ(H_2O_2) = x_{OH-OH}G^\circ_2(H_2) \quad (15)$$

$$G^\circ(OH^-) = G^\circ_1(H_2) \quad (16)$$

which implies that the initial G-values of H, OH, and the molecular products are temperature dependent. At room temperature we obtained $G^\circ(OH) = 5.48$ or 5.45 for $x_{OH-OH} = 0.5$ or 1.0, respectively, $G^\circ(H) = 0.33$, and $G^\circ(H_2) = 0.20$. These values are very similar to those assumed by LaVerne and Pimblott.[14]

Initial Spur Radii r°. The initial products are formed with greater than thermal energies. They dissipate their excess kinetic energy in random collisions with surrounding molecules in the thermalization process. To describe an inhomogeneous distribution of the hydrated electrons within the spur, three distribution functions of the thermalization distance have been considered:

$$\text{Gaussian } g(r_{th}) = (2\pi\sigma^2)^{-3/2} \exp[-r^2_{th}/(2\sigma^2)] \quad (17)$$

$$\text{Exponential } g(r_{th}) = (8\pi\sigma^3)^{-1} \exp(-r_{th}/\sigma) \quad (18)$$

$$\text{Trumbore central minimum}^{28} \quad g(r_{th}) = r^3_{th}/(32\pi\sigma^6) \exp[-r^2_{th}/(2\sigma^2)] \quad (19)$$

The parameter σ in eqs 17−19 characterizes the spatial extent of electrons in the spur and is called here the initial radius $r°_e$. The same distribution functions as for e_{aq}^- have been assumed for the products of the dissociative attachment of subexcitation electrons (process III). Although the spatial distribution of the captured electrons is expected to be narrower than that of the thermalized electrons,[41] the value of its width parameter has been found to be not very crucial and so it is equated with σ in eqs 17−19.

In the thermalization process the primary species are assumed to perform a random walk as they collide with surrounding water molecules. The number, n, of collisions occurring in a sphere of radius r_{th} can be related to the density, ϱ, of the system as follows:

$$n = Br_{th}^3\varrho \quad (20)$$

where B includes the reciprocal of the molecular mass of water and of Avogadro's number. The thermalization distances of the other species have been assumed to conform to the Gaussian distribution with $r_i° = r°$ for $i = H^+$, H, OH, H_2, and H_2O_2.

As no change in the energy deposition is expected, we assume that on average n does not depend on temperature. Because the density of the pressurized water decreases with increasing temperature,[49] this condition implies an increase in r_{th} at elevated temperatures according to

$$r_{th}(t) = r_{th}(25\ °C)[\varrho(25\ °C)/\varrho(t)]^{1/3} \quad (21)$$

where the ratio n/B is expressed by the product $r_{th}^3(25\ °C)\varrho(25\ °C)$. In eq 21 the thermalization distance at temperature t is a function of $r_{th}(25\ °C)$. Using the well-known formula

$$f(y) = g(x(y))|dy/dx| \quad (22)$$

with $y = r_{th}(t)$ and $x = r_{th}(25\ °C)$ and including a term r_{th}^2 omitted in eqs 17−19, it can be easily shown that the distribution function of $r_{th}(t)$ is expressed by that assumed for the room temperature case with the parameter σ multiplied by $[\varrho(25\ °C)/\varrho(t)]^{1/3}$. In consequence the parameters $r°_e$ and $r°$ have been scaled with temperature according to the density $\varrho(t)$ as follows:

$$r°_e = r°_e(25\ °C)[\varrho(25\ °C)/\varrho(t)]^{1/3} \quad (23)$$

The room temperature values of $r°(25\ °C)$ and $r°_e(25\ °C)$ have been obtained for each distribution by fitting the calculated G-values to the observed ones at $t = 25$ °C. The use of eq 23 results in $r°_e$ increasing by no more than 11.5% up to 300 °C compared with more than 150% in the model employed by LaVerne and Pimblott.[12]

Results and Discussion

Systematic measurements of the yields of radiolytic products in water have been recently performed by Elliot *et al.*[1] and Kent *et al.*[50] The criterion for a consistent set of the G-values is the material balance equation:

$$G_{red} = G_{ox} \quad (24)$$

where $G_{red} = G(e_{aq}^-) + G(H) + 2G(H_2)$ and $G_{ox} = G(OH) + 2G(H_2O_2)$. The data for G(OH) from ref 1 have been increased by 5% because the thiocyanate dosimeter system used to evaluate $G(OH)$[1] has recently been recalibrated.[51] Good agreement has been found between calculated and experimental values up to 300 °C. Our calculations confirmed that the spur reactions are complete and the radiolytic products diffuse out of the spur within 10^{-6} s. The differences between the G-values at 10^{-6} and 10^{-5} s do not exceed 1%. The G-values calculated at 10^{-6} s are compared with the experimental data in Figures 5 and 6 for the reducing and oxidizing products, respectively. Our results fit the experimental data well for both the reducing and oxidizing species. In the early stages of the spur processes, the decays of e_{aq}^- (Figure 7) and OH (Figure 8) are accelerated by increasing temperature. This is particularly evident for the electron. Later the probability of diffusion into the bulk increases and the decays become slower. The thermally dependent recombination probability of the dissociation fragments (H and OH) and the MHC result in an increase in the initial yield of OH at elevated temperatures.

As there are no data reported for the decays of e_{aq}^- and OH at high temperatures, our results are compared with experiment at 25 °C only. It should be noted here that the diffusion-kinetic models have been regarded as failing to fit both the experi-

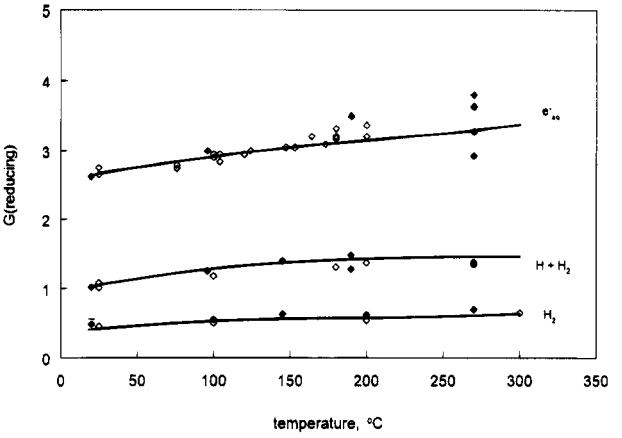

Figure 5. G-values of the reducing species calculated for the Gaussian distribution of e_{aq}^-. The experimental points are from ref 1 (◇) and from ref 50 (◆).

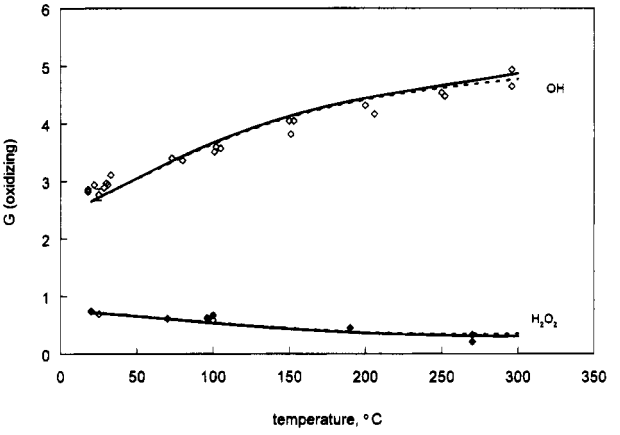

Figure 6. G-values of the oxidizing species calculated for the Gaussian distribution of e_{aq}^- and $x_{OH-OH} = 0.5$ (solid lines) or 1.0 (broken lines) (see text). The experimental points are from ref 1 (◇) and from ref 50 (◆).

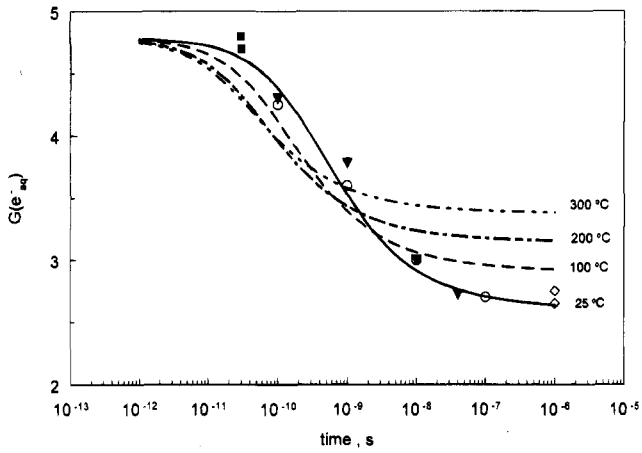

Figure 7. Decay of the hydrated electron in spur reactions as a function of temperature: (■) experimental data[54] for 25 °C; (○) data[55] derived from scavenged yields of e_{aq}^- measured in steady-state experiments; (▼) data[52] recalculated with the molar absorption coefficient reported by Elliot and Ouellette; (◇) data from ref 1.

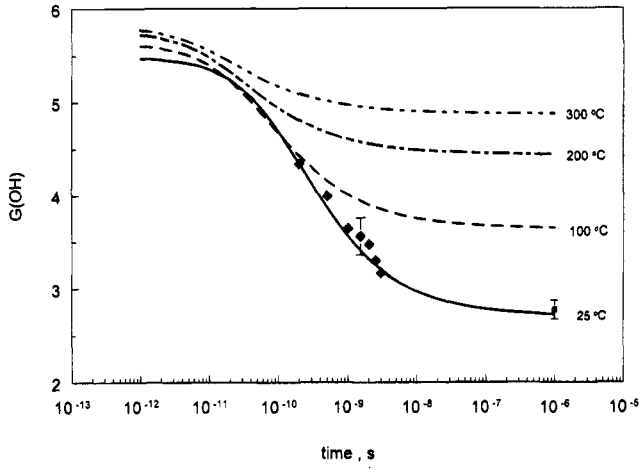

Figure 8. Decay of the hydroxyl radical in spur reactions as a function of temperature: (■) experimental data[1] for 25 °C; (◆) data estimated on the basis of the relative decay reported by Jonah *et al.*[56]

mentally observed decays and the absolute yields of e_{aq}^- and OH.[13,15] In particular, they predict too fast a decay of e_{aq}^- in comparison with the kinetics reported by Jonah *et al.*[52] In Figure 7 the data of Jonah *et al.*[52] have been recalculated with the molar absorption coefficient of 2×10^4 dm^3 mol^{-1} cm^{-1} recently reported by Elliot and Ouellette[9] instead of the previously accepted value of 1.85×10^4 dm^3 mol^{-1} cm^{-1} determined by Fielden and Hart[53] and now match the calculated yields reasonably well.

In Figure 9 the contributions of the spur reactions leading to the decay of e_{aq}^- are shown as a function of temperature. Up to 100 °C about 50% of electrons decay in the reaction with the OH radical (R2) and about 25% in the reaction with protons (R1). The contribution of the electron decay in the self reaction R4 becomes significant above 100 °C. It shows a broad maximum at 200 °C and makes the largest contribution up to 300 °C. The total contribution of reactions R5 and R9 does not exceed 10%.

The decay and formation of OH radicals is illustrated in Figure 10. In the whole temperature range the self reaction R8, which gives hydrogen peroxide as the product, and reaction R2 are responsible for the decay of the hydroxyl radicals. The contribution of reaction R9 in which an OH radical is formed and H_2O_2 decays is very small.

The modeling described above has been performed for the Gaussian distribution assumed as an initial spatial distribution

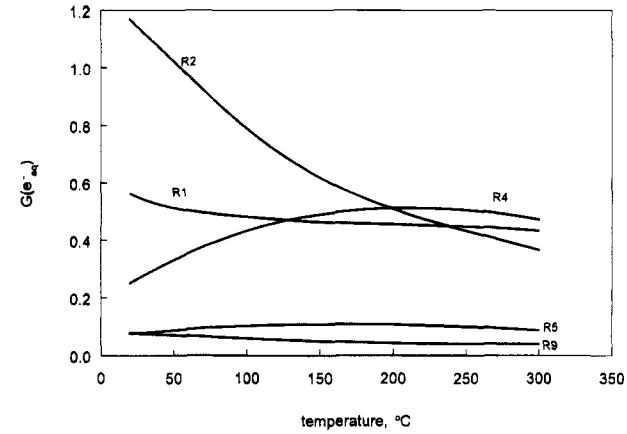

Figure 9. Contribution of spur reactions listed in Table 1 in the decay of the hydrated electron as a function of temperature.

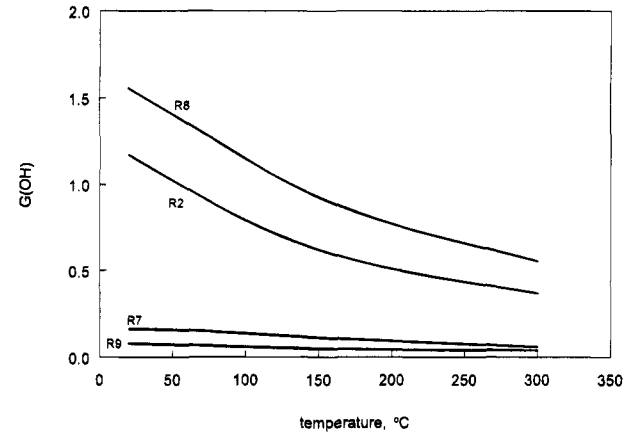

Figure 10. Contribution of spur reactions in the decay (reactions R2, R7, and R8) and formation (reaction R9) to the hydroxyl radical.

of the hydrated electrons. To check the effect of changing the distribution, the calculations have also been performed for exponential (eq 18) and central minimum (eq 19) distribution functions. The best fit to the experimental yields at room temperature has been found with the width parameters r°_e and r° equal to 2.3 and 0.85 nm, 1.3 and 0.86 nm, and 1.5 and 0.86 nm for the Gaussian, exponential, and central minimum distribution, respectively. The first pair of values are the same as used by LaVerne and Pimblott.[12,14] Our calculations show that the computed yields are independent of the function which describes the spatial distribution of e_{aq}^- within the spur. The relative differences in the *G*-values are below 3% and decrease with increasing temperature.

Summary

It is shown here that the "average" spur model[13-15] is applicable for the description of the chemical stage in pressurized water up to 300 °C. In the absence of scavengers the chemical stage is complete in 10^{-6} s. Calculations show that the yields at this stage are independent of the spatial distribution assumed for the hydrated electron over the whole temperature range. To account for an unscavengeable yield of H_2, both the dissociative attachment of subexcitation electrons to water and the decomposition of vibrationally and electronically excited states of water have been included in the modeling. The former process has been regarded as being independent of temperature, while an increase in the fragmentation channel $H_2O^* \rightarrow H_2 + O(^1D)$ from 4.5% at 25 °C to 18% at 300 °C has been shown to explain the observed increase in $G(H_2)$ above 210 °C. The contribution from this channel at 300 °C is consistent with the experimental data reported for the gas phase.

The most important spur reactions responsible for the decay of the OH radical are the bimolecular reaction OH + OH → H_2O_2 and reaction R2 with the hydrated electron. The decay of e_{aq}^- in its reactions with OH and the proton, which prevail at room temperature, becomes less important at 300 °C and comparable with that in the self reaction R4 ($e_{aq}^- + e_{aq}^- \rightarrow H_2 + 2OH^-$). Reaction R4 is mainly responsible for the creation of molecular hydrogen within the spur. This reaction is postulated as diffusion controlled at elevated temperatures. The calculated yields of radiolytic products cover the measured values within experimental error over the whole temperature range.

Acknowledgment. D.S. thanks the Commission of the European Communities for a Research Fellowship. We are grateful to Dr. W. G. Burns and Dr. A. J. Elliot for helpful and encouraging discussions.

References and Notes

(1) Elliot, A. J.; Chenier, M. P.; Ouellette, D. C. *J. Chem. Soc., Faraday Trans.* **1993**, *89*, 1193.
(2) Mozumder, A.; Magee, J. L. *J. Chem. Phys.* **1966**, *45*, 332.
(3) Mozumder, A.; Magee, J. L. *Radiat. Res.* **1966**, *28*, 215.
(4) Elliot, A. J. *Radiat. Phys. Chem.* **1989**, *34*, 753.
(5) Elliot, A. J.; McCracken, D. R.; Buxton, G. V.; Wood, N. D. *J. Chem. Soc., Faraday Trans.* **1990**, *86*, 1539.
(6) Buxton, G. V.; Elliot, A. J. *J. Chem. Soc., Faraday Trans.* **1993**, *89*, 485.
(7) Natzle, W. C.; Moore, C. B. *J. Phys. Chem.* **1985**, *89*, 2605.
(8) Sehested, K.; Christensen, H. *Radiat. Phys. Chem.* **1990**, *36*, 499.
(9) Elliot, A. J.; Ouellette, D. C. *J. Chem. Soc., Faraday Trans.* **1994**, *90*, 837.
(10) Christensen, H.; Sehested, K. *J. Phys. Chem.* **1986**, *90*, 186.
(11) Christensen, H.; Sehested, K.; Logager, T. *Radiat. Phys. Chem.* **1994**, *43*, 527.
(12) LaVerne, J. A.; Pimblott, S. M. *J. Phys. Chem.* **1993**, *97*, 3291.
(13) Burns, W. G.; Sims, H. E.; Goodall, J. A. B. *Radiat. Phys. Chem.* **1984**, *23*, 143.
(14) LaVerne, J. A.; Pimblott, S. M. *J. Phys. Chem.* **1991**, *95*, 3196.
(15) Pimblott, S. M.; LaVerne, J. A. *Radiat. Res.* **1990**, *122*, 12.
(16) Schwarz, H. A. *J. Phys. Chem.* **1969**, *73*, 1928.
(17) (a) Bisby, R. H.; Burns, W. G.; Cundall, R. B.; Sims, H. E. *Faraday Discuss. Chem. Soc.* **1975**, *63*, 237. (b) Burns, W. G.; Sims, H. E. *J. Chem. Soc., Faraday Trans. 1* **1981**, *77*, 2803.
(18) Chance, E. M.; Curtis, A. R.; Jones, T. P.; Kirby, C. R. AERE Report. AERER8775; H.M.S.O.: 1977.
(19) Miller, D. G. Lawrence Livermore National Laboratory Report 53319; 1982.
(20) Quist, A. S.; Marshall, W. L. *J. Phys. Chem.* **1965**, *69*, 2984.
(21) Weingartner, H. *Z. Phys. Chem.* **1982**, *132*, 128.
(22) Barker, G. C.; Fowles, P.; Sammon, D. C.; Stringer, B. J. *J. Chem. Soc., Faraday Trans. 1* **1970**, *66*, 1998.
(23) Buxton, G. V.; Greenstock, C. L.; Helman, W. P.; Ross, A. B. *J. Phys. Chem. Ref. Data* **1988**, *17*, 813.
(24) Noyes, R. M. In *Progress in Reaction Kinetics*; Porter, G., Ed.; Pergamon Press: London, 1961; p 129.
(25) Akerlof, G. C.; Oshry, H. I. *J. Am. Chem. Soc.* **1950**, *72*, 2844.
(26) Schwarz, H. A. *J. Phys. Chem.* **1992**, *96*, 8937.
(27) Matheson, M. S.; Rabani, J. *J. Phys. Chem.* **1965**, *69*, 1324.
(28) Trumbore, C. N.; Short, D. R.; Fanning, J. E.; Olsen, J. H. *J. Phys. Chem.* **1978**, *82*, 2762.
(29) Pimblott, S. M.; Mozumder, A. *J. Phys. Chem.* **1991**, *95*, 7291.
(30) Kaplan, I. G.; Sukhonosov, V. Y. *Radiat. Res.* **1991**, *127*, 1.
(31) Bugaenko, L. T.; Byakov, V. M.; Kabakchi, S. A. *Khim. Vys. Energ.* **1985**, *19*, 291.
(32) Kaplan, I. G.; Miterev, A. M.; Sukhonosov, V. Y. *Radiat. Phys. Chem.* **1990**, *36*, 493.
(33) Platzman, R. L. *Abstracts of Papers, Second International Congress of Radiation Research*, Harrogate, 5−11 August, 1962; Ebert, M., Howard, A., Eds.; North-Holland Publishing: Amsterdam, 1963; p 128.
(34) Faraggi, M.; Desalos, J. *Int. J. Radiat. Phys. Chem.* **1969**, *1*, 335.
(35) Claydon, C. R.; Segal, G. A.; Taylor, H. S. *J. Chem. Phys.* **1971**, *54*, 3799.
(36) Black, G.; Porter, G. *Proc. R. Soc. London* **1962**, *A266*, 185.
(37) Stief, L. J. *J. Chem. Phys.* **1966**, *44*, 277.
(38) Slanger, T. G.; Black, G. *J. Chem. Phys.* **1982**, *77*, 2432.
(39) Mul, P. M.; McGowan, J. W.; Defrance, P.; Mitchell, J. B. A. *J. Phys. B: At. Mol. Phys.* **1983**, *16*, 3099.
(40) Brown, W. G.; Hart, E. J. *J. Phys. Chem.* **1978**, *82*, 2539.
(41) Goulet, T.; Patau, J.-P.; Jay-Gerin, J.-P. *J. Phys. Chem.* **1990**, *94*, 7312.
(42) Burns, W. G.; Marsh, W. R. *J. Chem. Soc., Faraday Trans. 1* **1981**, *77*, 197.
(43) Biedenkapp, D.; Hartshorn, L. G.; Bair, E. J. *J. Chem. Phys. Lett.* **1970**, *5*, 379.
(44) Taube, H. *Trans. Faraday Soc.* **1957**, *53*, 656.
(45) Buxton, G.; Wilmarth, W. K. *J. Phys. Chem.* **1963**, *67*, 2835.
(46) Welge, K. H.; Stuhl, F. J. *Chem. Phys.* **1967**, *46*, 2440.
(47) Sengers, J. V.; Watson, J. T. R. *J. Phys. Chem. Ref. Data* **1986**, *15*, 1302.
(48) Bagdasaryan, K. S. *Russ. Chem. Rev.* **1984**, *53*, 623.
(49) Dorsey, N. E. *Properties of Ordinary Water Substance in all its Phases*; Reinholt Publishing Corp.: New York, 1940; p 583.
(50) Kent, M. C.; Sims, H. E. 6th International Conference on Water Chemistry of Nuclear Reactor Systems, October 1992; British Nuclear Energy Society: London, 1992; Vol. 2, p 322.
(51) Buxton, G. V.; Stuart, C. R. *J. Chem. Soc., Faraday Trans.* **1995**, *91*, 279.
(52) Jonah, C. D.; Matheson, M. S.; Miller, J. R.; Hart, E. J. *J. Phys. Chem.* **1976**, *80*, 1267.
(53) Fielden, E. M.; Hart, E. J. *Radiat. Res.* **1967**, *32*, 564.
(54) (a) Sumiyoshi, T.; Katayama, M. *Chem. Lett.* **1982**, 1887. (b) Sumiyoshi, T.; Tsugaru, K.; Yamada, T.; Katayama, M. *Bull. Chem. Soc., Jpn.* **1985**, *58*, 3073.
(55) Balkas, T. I.; Fendler, J. H.; Schuler, R. H. *J. Phys. Chem.* **1970**, *74*, 4497.
(56) Jonah, C. D; Miller, J. R. *J. Phys. Chem.* **1977**, *81*, 1974.

JP9513780